

## Supporting Information

Hollow Au-Cu<sub>2</sub>O core-shell nanoparticles with geometry-dependent optical properties as efficient plasmonic photocatalysts under visible light

*Biao Lu,<sup>†</sup> Aiping Liu,<sup>\*,†,‡</sup> Huaping Wu,<sup>§</sup> Qiuping Shen,<sup>†</sup> Tingyu Zhao<sup>†</sup> and Jianshan Wang<sup>||</sup>*

<sup>†</sup>Center for Optoelectronics Materials and Devices, Zhejiang Sci-Tech University, Hangzhou 310018, China

<sup>‡</sup>State Key Laboratory of Nonlinear Mechanics, Institute of Mechanics, Chinese Academy of Sciences, Beijing 100190, China

<sup>§</sup>Key Laboratory of E&M (Zhejiang University of Technology), Ministry of Education & Zhejiang Province, Hangzhou 310014, China

<sup>||</sup>Tianjin Key Laboratory of Modern Engineering Mechanics, Department of Mechanics, Tianjin University, Tianjin 300072, China

\*Corresponding author. Tel.: +86 571 86843574; fax: +86 571 86843574.

E-mail address: liuaiping1979@gmail.com.

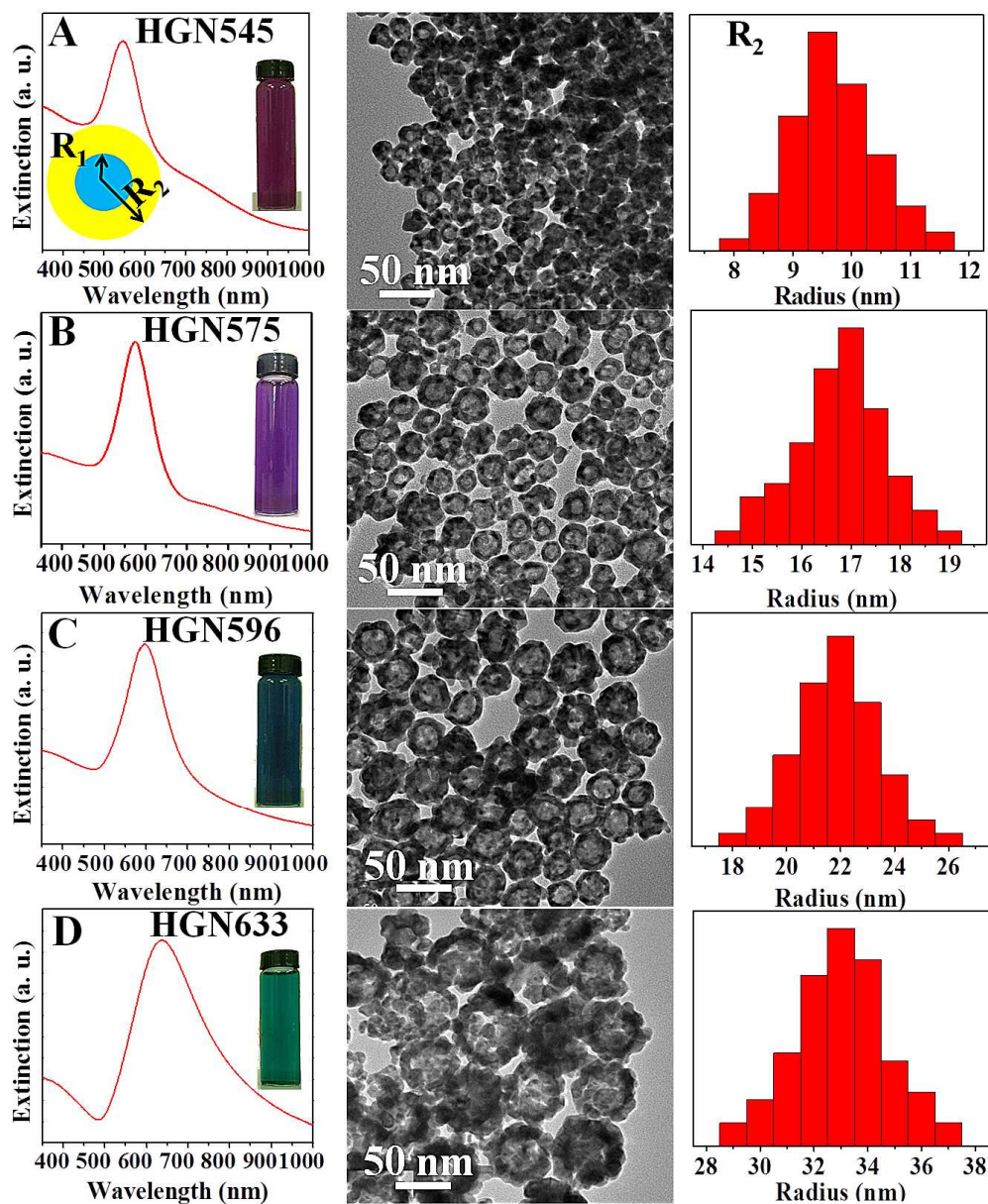


Figure S1 Extinction spectra and corresponding photographs of hollow gold nanoparticle (HGN) colloids, TEM images and size distribution histograms of HGNs with different sizes: (A) HGN545, (B) HGN575, (C) HGN596 and (D) HGN633. The HGN samples are named with the position of surface plasmon resonance (SPR) peaks at the extinction spectra. The geometry of the HGNs is assumed to be a concentric two-layered sphere with the cross-sectional drawing shown in (A).  $R_1$  and  $R_2$  are the average inner radius and outer one.

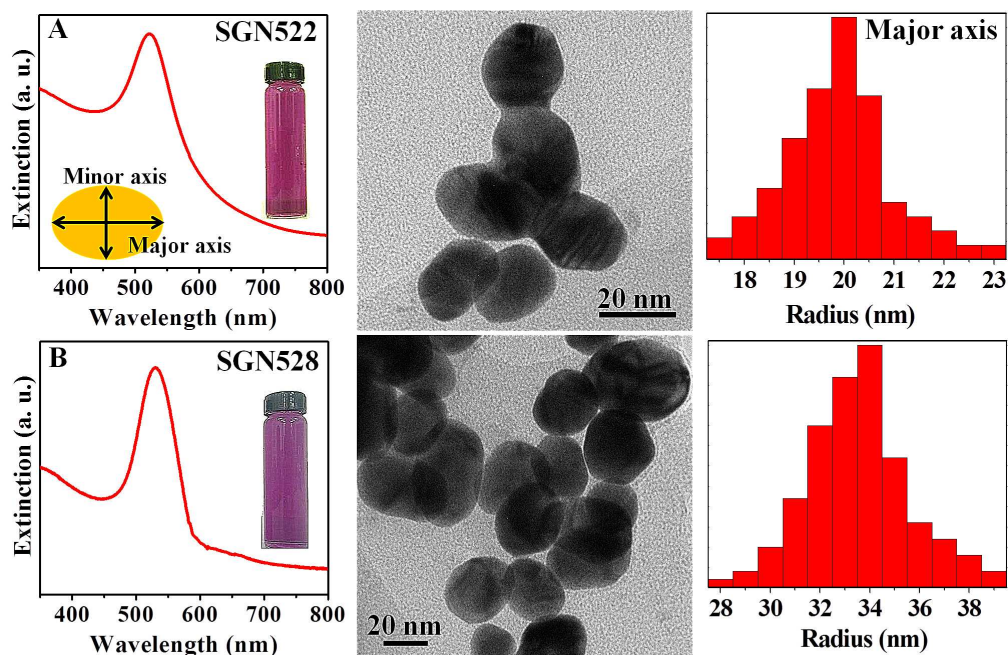


Figure S2 Extinction spectra and corresponding photographs of solid gold nanoparticle (SGN) colloids, TEM images and size distribution histograms of SGNs with different sizes: (A) SGN522 and (B) SGN528. The SGN samples are named with the position of SPR peaks at the extinction spectra. The geometry of the SGNs is assumed to be ellipsoidal with the cross-sectional drawing shown in (A).

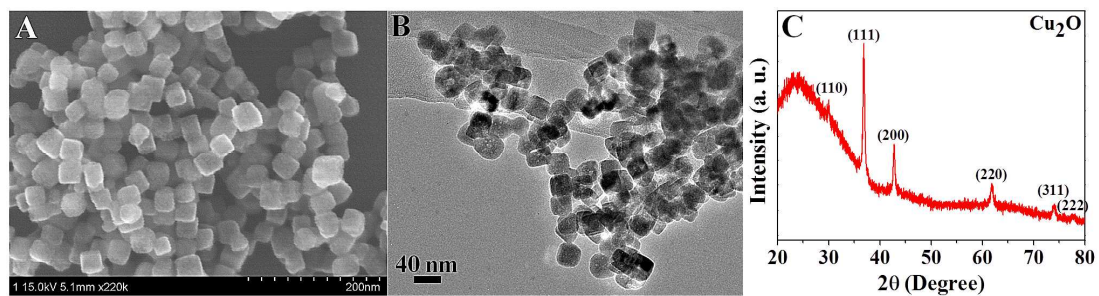


Figure S3 (A) SEM image, (B) TEM image and (C) XRD pattern of pristine Cu<sub>2</sub>O truncated nanocubes. The structure-directing agent is polyethylene glycol (PEG).

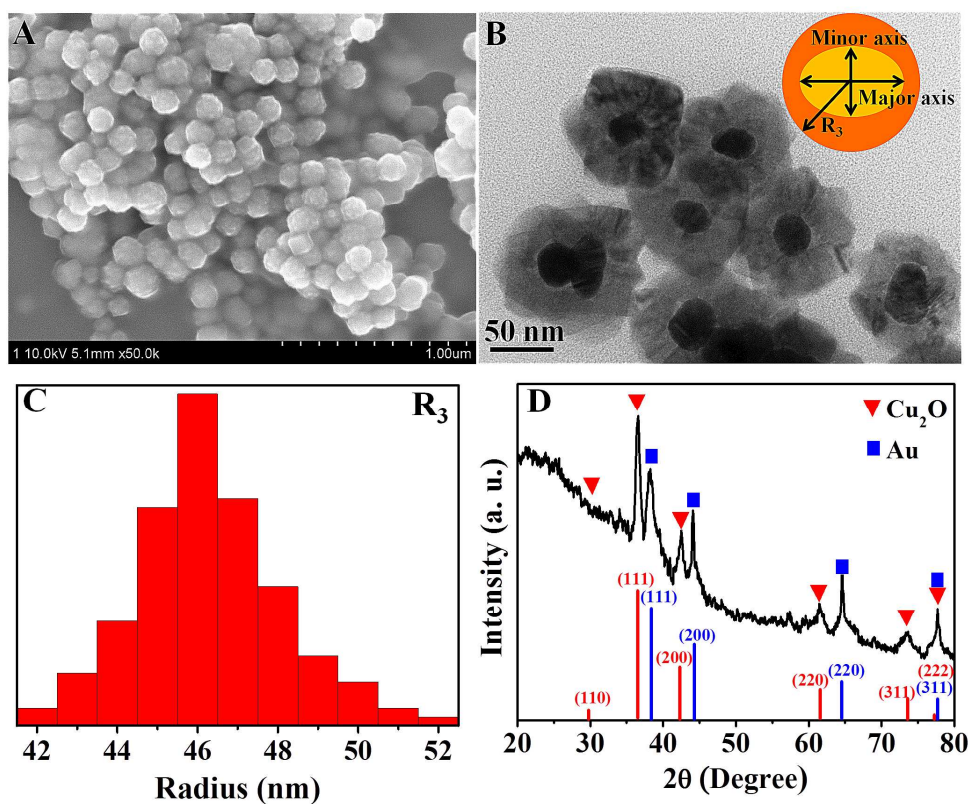


Figure S4 (A) SEM image, (B) TEM image, (C) size distribution histogram and (D) XRD pattern of solid Au-Cu<sub>2</sub>O core-shell nanoparticles. The SGN528 is used as the core and the structure-directing agent is PEG. The scheme of cross-sectional drawing of the nanoparticle is shown in (B).  $R_3$  is the average outer radius of the nanoparticle. Red lines and blue lines in (D) represent the standard diffraction data of face-centered cubic crystalline Cu<sub>2</sub>O and gold, respectively.



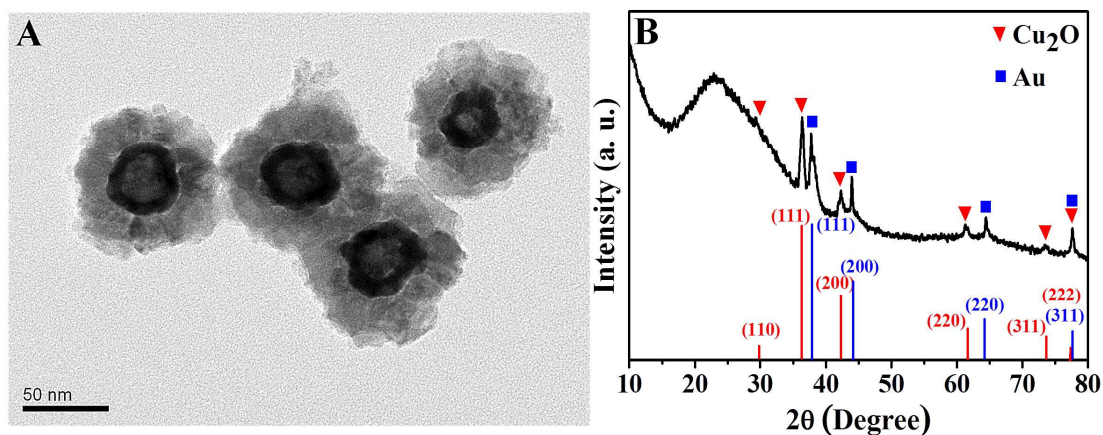


Figure S5 (A) TEM image of hollow Au-Cu<sub>2</sub>O core-shell nanoparticles with HGN596 as the core and Cu<sub>2</sub>O shell thickness about 20 nm. The structure-directing agent is PVP. (B) XRD pattern of hollow Au-Cu<sub>2</sub>O core-shell nanoparticles in Figure 3C. Red lines and blue lines represent the standard diffraction data of face-centered cubic crystalline Cu<sub>2</sub>O and gold, respectively.

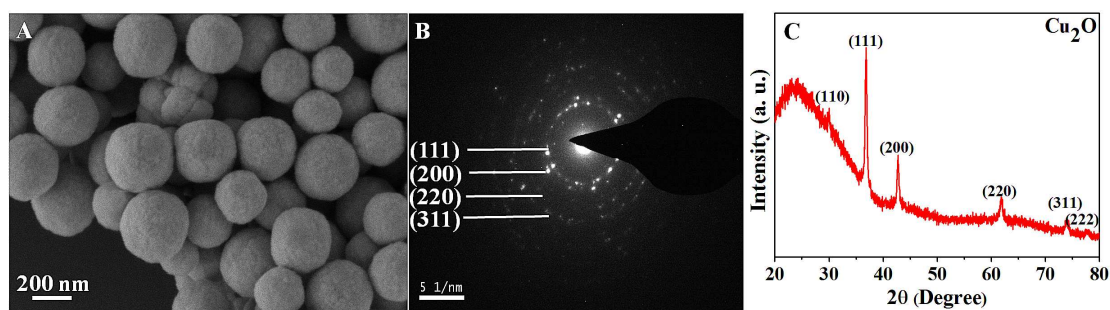


Figure S6 (A) SEM image, (B) SAED pattern and (C) XRD pattern of pristine Cu<sub>2</sub>O nanospheres. The structure-directing agent is PVP.

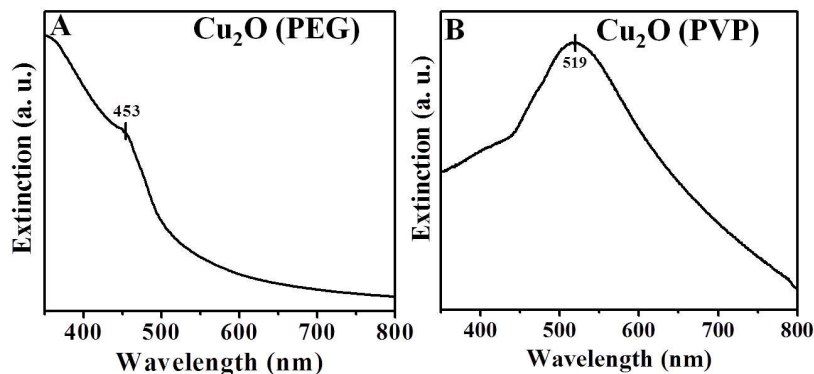


Figure S7 Extinction spectra of colloidal solutions of (A) pristine  $\text{Cu}_2\text{O}$  truncated nanocubes and (B) pristine  $\text{Cu}_2\text{O}$  nanospheres prepared by using PEG and PVP as the structure-directing agents, respectively.

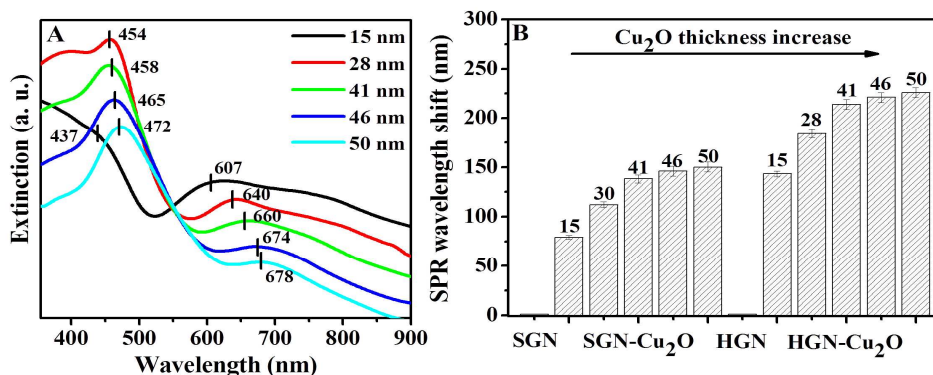


Figure S8 Experimental extinction spectra of solid Au- $\text{Cu}_2\text{O}$  core-shell nanoparticles with increasing  $\text{Cu}_2\text{O}$  thickness in the range from 15 nm to 50 nm. The average outer radius  $R_3$  of Au- $\text{Cu}_2\text{O}$  core-shell nanoparticles are  $32 \pm 1.5$  nm,  $45 \pm 2.0$  nm,  $57 \pm 2.2$  nm,  $63 \pm 2.5$  nm and  $67 \pm 2.8$  nm (from top to bottom). The SGN528 is used as the core and the structure-directing agent is PEG. (B) Plots summarizing the SPR band shifts of solid Au- $\text{Cu}_2\text{O}$  core-shell nanoparticles (Figure S8A) and hollow ones (Figure 4A) with respect to the  $\text{Cu}_2\text{O}$  thickness. The error bars present the standard deviations of SPR band shift determined by six UV-Vis absorption spectra for each sample.

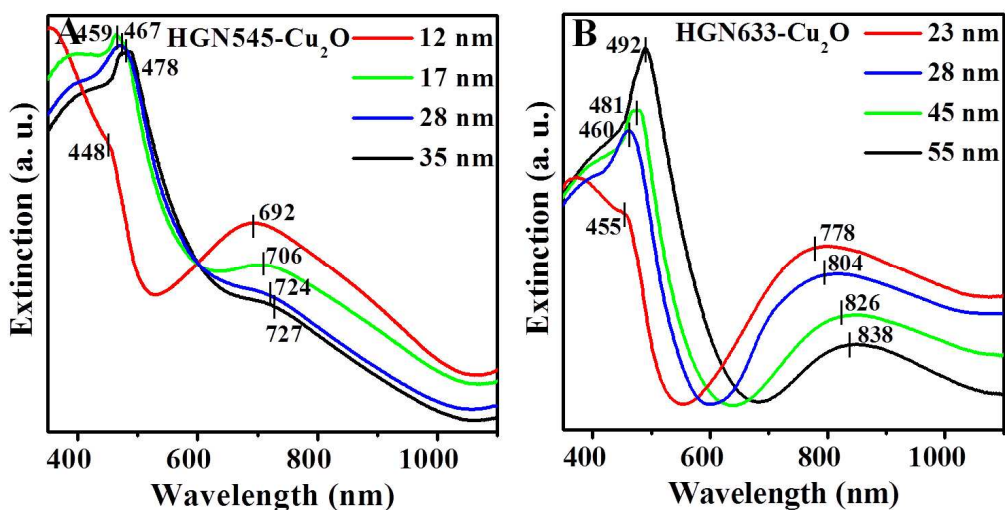


Figure S9 Experimental extinction spectra of hollow Au-Cu<sub>2</sub>O core-shell nanoparticles with different sizes of HGN cores: (A) HGN545 with increasing Cu<sub>2</sub>O thickness in the range from 12 nm to 35 nm (the average outer radius  $R_3$  are  $21 \pm 1.2$  nm,  $26 \pm 1.5$  nm,  $37 \pm 1.8$  nm and  $44 \pm 2.0$  nm from top to bottom), (B) HGN633 with increasing Cu<sub>2</sub>O thickness in the range from 23 nm to 55 nm (the average outer radius  $R_3$  are  $56 \pm 2.2$  nm,  $61 \pm 2.5$  nm,  $78 \pm 2.8$  nm and  $88 \pm 3.2$  nm from top to bottom). The structure-directing agent is PEG.

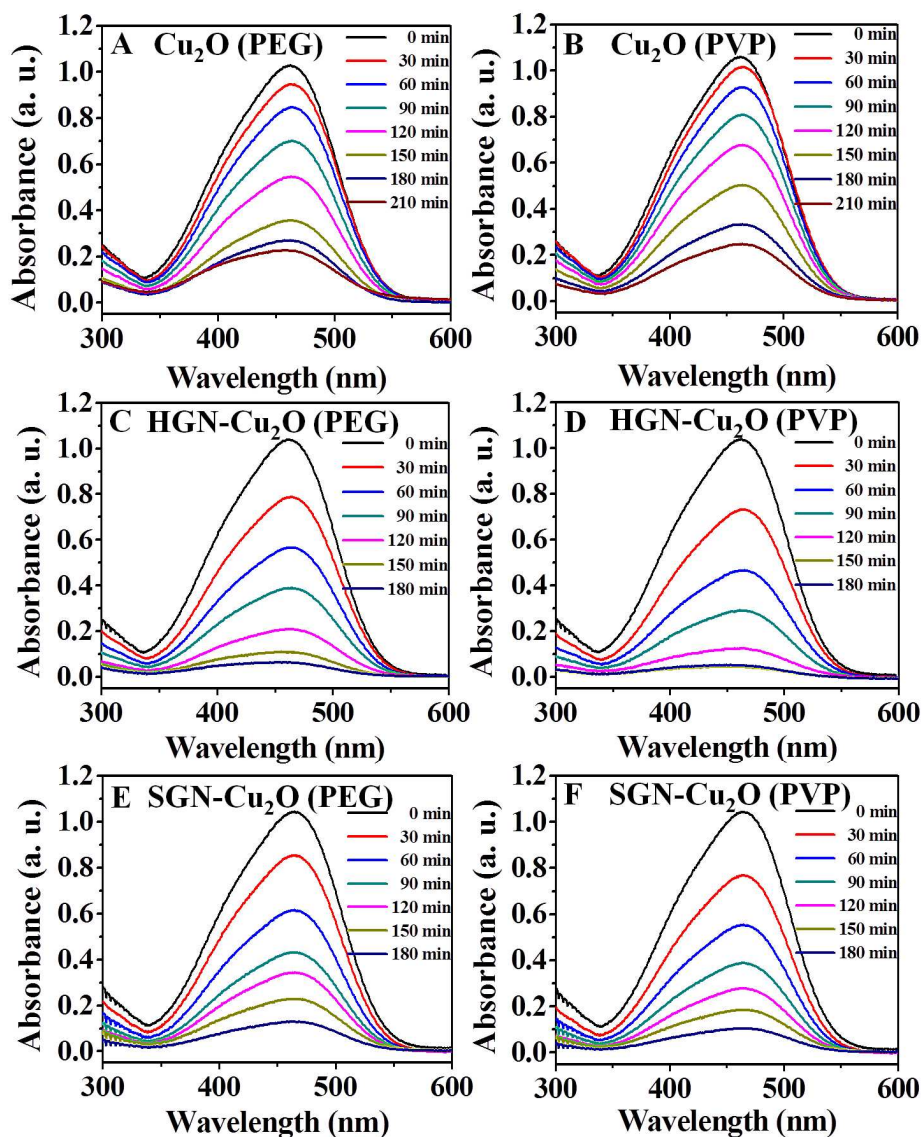


Figure S10 Variation in the extinction spectra of MO solution in the presence of different photocatalysts under visible-light irradiation for different irradiation times: (A)  $\text{Cu}_2\text{O}$  prepared with PEG, (B)  $\text{Cu}_2\text{O}$  prepared with PVP, (C) hollow Au- $\text{Cu}_2\text{O}$  core-shell nanoparticles prepared with PEG, (D) hollow Au- $\text{Cu}_2\text{O}$  ones prepared with PVP, (E) solid Au- $\text{Cu}_2\text{O}$  core-shell nanoparticles prepared with PEG and (F) solid Au- $\text{Cu}_2\text{O}$  ones prepared with PVP, respectively. The HGN575 and SGN528 are used as the cores and the  $\text{Cu}_2\text{O}$ -shell thicknesses are about 28 nm.



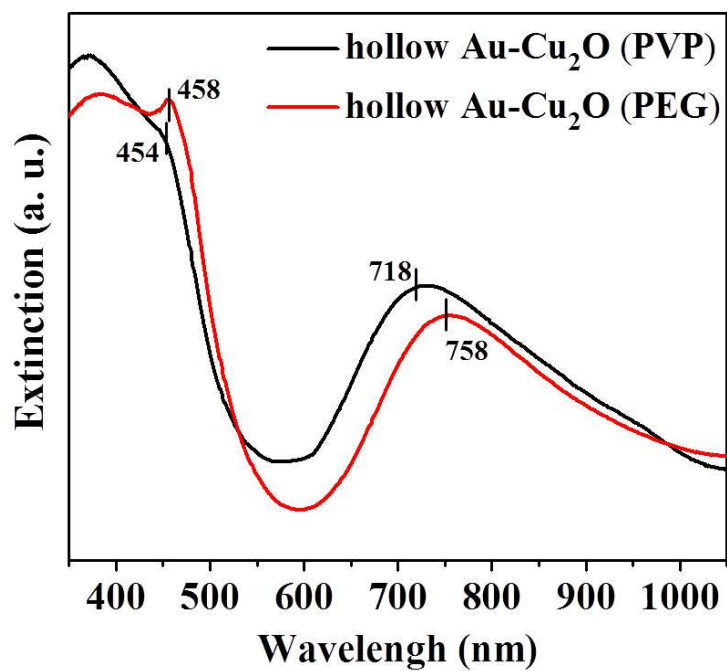


Figure S11 Experimental extinction spectra of hollow Au-Cu<sub>2</sub>O core-shell nanoparticles prepared with the structure-directing agents of PEG and PVP. The HGN575 is used as the cores and the thicknesses of Cu<sub>2</sub>O shell are about 28 nm.